

Heating Properties of the Needle Type Applicator Made of Shape Memory Alloy by 3-D Anatomical Human Head Model

N. Mimoto, K. Kato, Y. Kanazawa, Y. Shindo, K. Tsuchiya, M. Kubo, T. Uzuka, H. Takahashi and Y. Fujii

Abstract— Since the human brain is protected by the skull, it is not easy to non-invasively heat deep brain tumors with electromagnetic energy for hyperthermia treatments. Generally, needle type applicators were used in clinical practice to heat brain tumors. To expand the heating area of needle type applicators, we have developed a new type of needle made of a shape memory alloy (SMA). In this paper, heating properties of the proposed SMA needle type applicator were discussed. Here, in order to apply the SMA needle type applicator clinically. First, we constructed an anatomical 3-D FEM model from MRI and X-ray CT images using 3D-CAD software. Second, we estimated electric and temperature distributions to confirm the SMA needle type applicator using the FEM soft were JMAG-Studio. From these results, it was confirmed that the proposed method can expand the heating area and control the heating of various sizes of brain tumors.

I. INTRODUCTION

As the human brain is protected by the skull, it is not easy to heat deep brain tumors non-invasively with electromagnetic energy for hyperthermia treatments. Several heating methods have been proposed to heat deep tumors. Some examples are radio frequency (RF) capacitive heating applicators [1], annular phased applicators [2], and coaxial transverse electromagnetic (TEM) applicators [3]. Some of these methods have been in practical use. However, all of them have advantages and disadvantages, and a successful heating method has not yet been realized. Typically, the radio frequency (RF) interstitial hyperthermia system with a needle type applicator is used in clinical practice to invasively heat malignant brain tumors [4], [5]. However, this method has both the advantages and disadvantages. One of the advantages is that direct and local heating of the area around the needle is possible. Disadvantages are that this heating method has a small heating area and is an invasive heating method. To overcome these problems, in 1989 the authors proposed a heating method using two or more needle type electrodes. However, the burden to the patient is large, and in order to carry out effective heating, it is indispensable. Further, it is not easy for a medical doctor to set two or more parallel needles in parallel inside a brain tumor.

N. Mimoto, K. Kato, Y. Kanazawa, Y. Shindo, and K. Tsuchiya are with the Department of Mechanical Engineering Informatics, Meiji University, Kawasaki, Japan (e-mail: ce92065@isc.meiji.ac.jp).

M. Kubo is with the Future Creation Laboratory, Olympus Co., Ltd., Tokyo, Japan.

H. Takahashi is with the Niigata Cancer Center Hospital, Niigata, Japan.

T. Uzuka and Y. Fujii are with the Department of Neurosurgery, Brain Research Institute, Niigata University, Niigata, Japan.

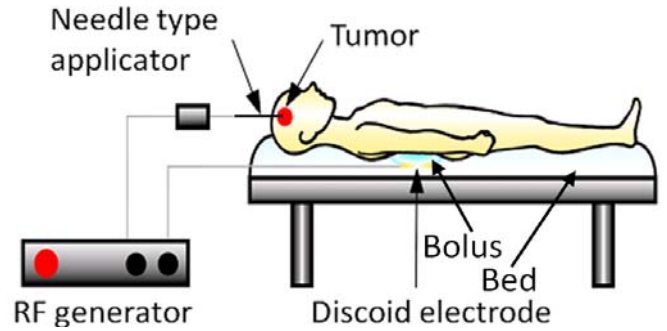


Fig. 1. Illustration of heating system.

In order to expand the heating area of a needle type applicator, we have developed a new type of needle made of a shape memory alloy (SMA). The needle type electrode used in the clinic was made by stainless steel.

II. METHODS

An illustration of our heating system is shown in Fig. 1. In Fig. 1, a needle type applicator, which is made of SMA, is inserted into the brain tumor and heated by a RF current between a needle applicator and a discoid electrode. So, the tissue around the needle is heated intensively.

The tissue temperature T in a human heated by the electromagnetic energy can be calculated by equations (1)-(6):

$$\rho c \frac{\partial T}{\partial t} = \nabla^2 (\kappa T) + W_h - W_c + M \quad (1)$$

$$W_h = \frac{1}{2} \sigma |E|^2 \quad (2)$$

$$\nabla \cdot [(\sigma + j\omega \epsilon_r \epsilon_o) \nabla \phi] = 0 \quad (3)$$

$$E = -\text{grad} \phi \quad (4)$$

$$W_c = (F\rho)_{\text{tissue}} \times (\rho c)_{\text{blood}} \times (T - T_b) \quad (5)$$

$$M = M_0 (1.1)^{\Delta T} \quad (6)$$

Where ρ is the volume density of tissue, c is the specific heat of tissue, κ is the thermal conductivity, W_h is the heating energy generated by the high-frequency current in a human head, W_c is the cooling energy by the blood flow, and M is the metabolic heat generation. σ is the electrical conductivity, ϕ is the electrical potential, ω is the radial frequency, ϵ_r is the relative dielectric constant, ϵ_o is the permittivity of free space, μ is the magnetic permeability,

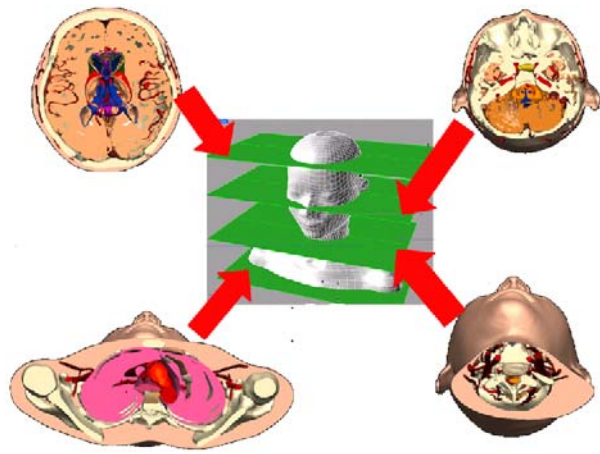


Fig. 2 . Method of reconstructing 3-D human head model.

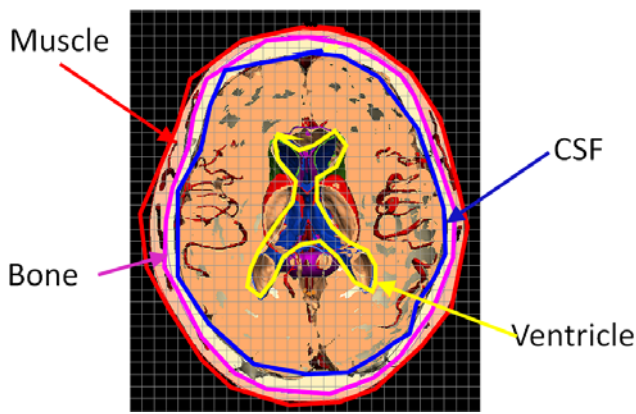


Fig. 3. Traced contours.

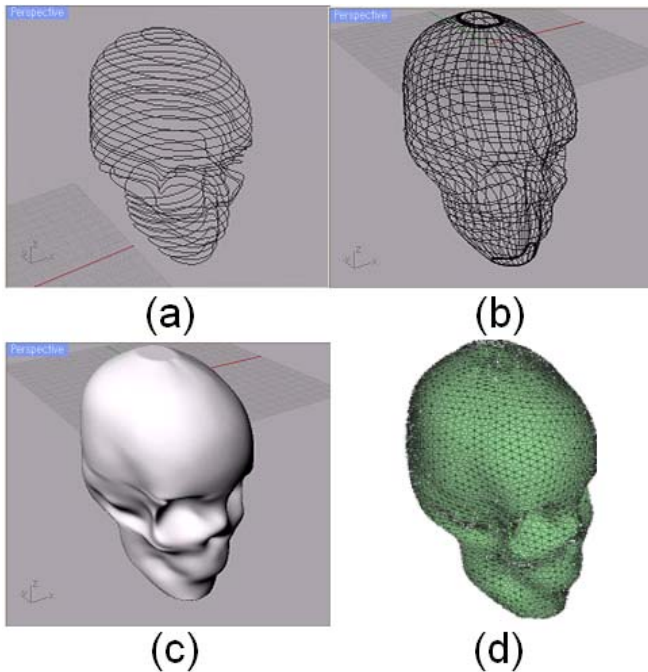


Fig. 4. Extracted tissues and the FEM mesh model; (a) Collected contours, (b) Surface model, (c) Solid model, (d) FEM models.

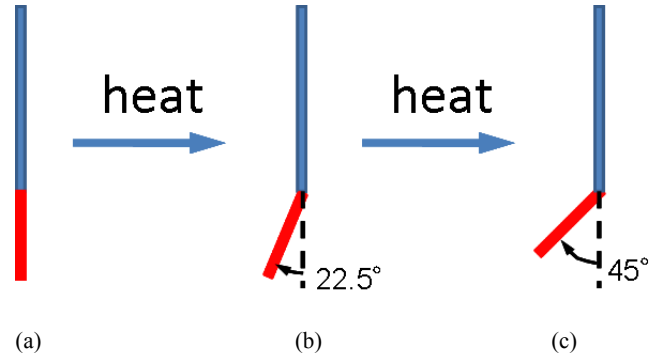


Fig. 5. Shape changes of SMA.

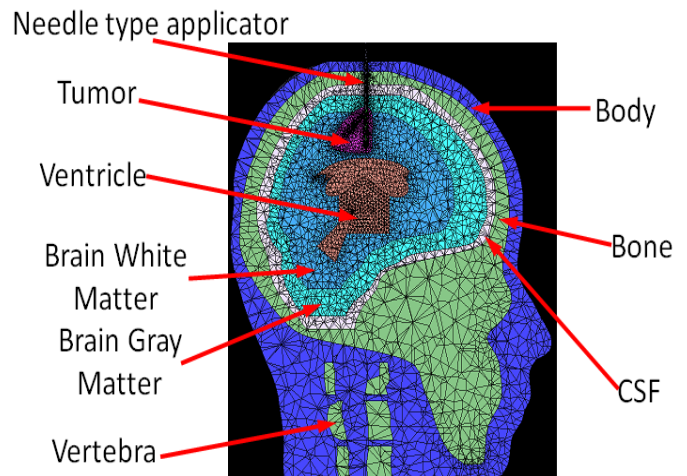


Fig. 6. FEM mesh model.

F is the blood flow rate, T_b is the blood temperature, $\Delta T = T - T_{Mo}$, T_{Mo} is the basal metabolic temperature, and M_o is the basal metabolic heat generation rate respectively[1]. Equations (1) and (3) can be solved numerically by the finite element method (FEM). In this study, we assume that the center of tumor has few blood flow, therefore, the heating area is close to the center of tumor.

III. ANALYTICAL MODEL

Our purpose is to reconstruct the 3-D anatomical model from MRI images and CTs and to show by computer simulations that the needle type applicator made of SMA may apply to clinical heating.

Fig. 2 shows a method of reconstructing the 3-D human head model. Our reconstruction method of the 3-D anatomical model consists of five steps.

The first step is to collect the standard MRI images as shown in Fig. 2 from Virtual Anatomy.

TABLE I
Electromagnetic Properties of the Tissues at 13.56MHz

Tissue	σ [S/m]	ϵ	ρ [kg/m ³]
Tumor(muscle)	0.62818	138.44	1,040
Verticle(CSF)	2.0041	108.26	1,010
Brain White Matter	0.17563	153.12	1,030(Brain ave)
Brain Grey Matter	0.32737	263.38	1,030(Brain ave)
Cerebro Spinal Fluid(CSF)	2.0041	108.26	1,010
Bone Marrow	0.012905	16.058	1,810
Muscle	0.62818	138.44	1,040
Heart	0.52617	239.13	1,040(Muscle)
Needle electrode	13×10^6	-	6,942
Discoid electrode	59×10^6	-	8,920
Water	0.047	-	-

TABLE II
Thermal Properties of the Tissue at 36.8°C

Tissue	C[J/kg°C]	κ [W/m°C]
Tumor(muscle)	3,650	0.5
Verticle(CSF)	3,802	0.57
Brain White Matter(brain ave.)	3,672	0.528
Brain Grey Matter(brain ave.)	3,672	0.528
Cerebro Spinal Fluid(CSF)	3,802	0.57
Bone Marrow	1,440	0.36
Muscle	3,650	0.5
Heart(muscle)	3,650	0.5
Needle electrode	463	83
Discoid electrode	380	390
Water	-	-

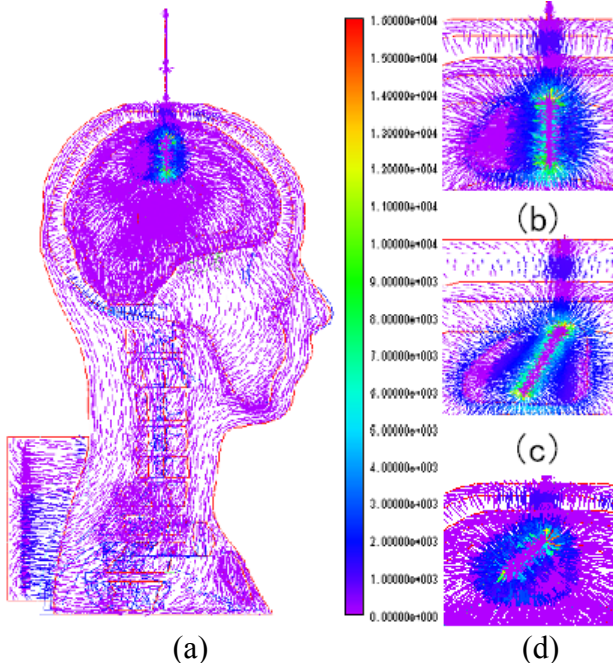


Fig. 7. Results of electric current distributions;
(a)overall distribution,

(b)close-up distribution around the needle(bend angle: 0°),
(c)close-up distribution around the needle(bend angle: 22.5°),
(d)close-up distribution around the needle(bend angle: 45°).

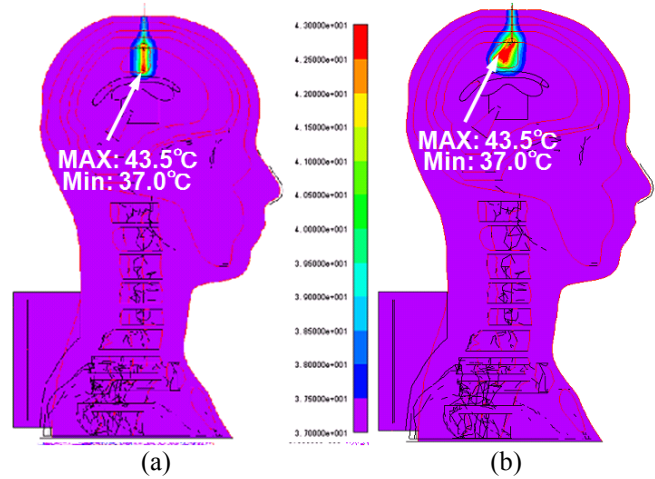


Fig. 8. Estimated temperature distributions
after 90 seconds of heating;
(a) bend angle 0°, (b) bend angle 0° -22.5° -45.0°.

The second step is to trace these tissues of contour shown in Fig. 3. Fig. 4 shows extracted tissues and the FEM mesh model. Fig. 5 shows the shape change images of the SMA.

The third step is to collect and combine these contours shown in Fig.4 (a) and Fig. 4(b).

The fourth step is to make solid models shown in Fig. 4(c) from the third step. From the second step to the fourth step, the commercial 3D-CAD software, Rhinoceros, was used.

The last step is to make the FEM models shown in Fig. 5 (d). Fig. 6 is the solid models created by commercial pre-processor, Hyper Mesh.

Fig. 6 shows a FEM model for electric and temperature distributions. Here, the commercial FEM software, JMAG, was used in computer simulations. The physical parameters used in the calculations are listed in Table I and Table II [6].

We calculated the electric and temperature distributions of the needle type applicator made of SMA with the FEM mesh model shown in Fig. 6.

IV. RESULTS AND DISCUSSION

A. Analysis of electric current distribution

Fig. 7 shows the results of electric current distributions inside the human tissue calculated by the FEM. In Fig. 7(a), the electric current is concentrated around the needle electrode. There is no location in particular that the electric current is concentrated except the small area around the needle. Figs. 7(b), (c) and (d) show the electric current distributions around the needle electrodes bent to 0°, 22.5° and 45° angles. From Figs. 7(b), (c) and (d), it is found that the electric currents are distributed in accordance with the shape of needle the electrode.

B. Analysis of temperature distribution

Fig. 8 shows the results of the estimated temperature distributions by the FEM. Fig. 8(a) is estimated temperature distribution of the clinical type of needle applicator after 1 minute and 30 seconds heating. On the other hand, Fig. 8(b)

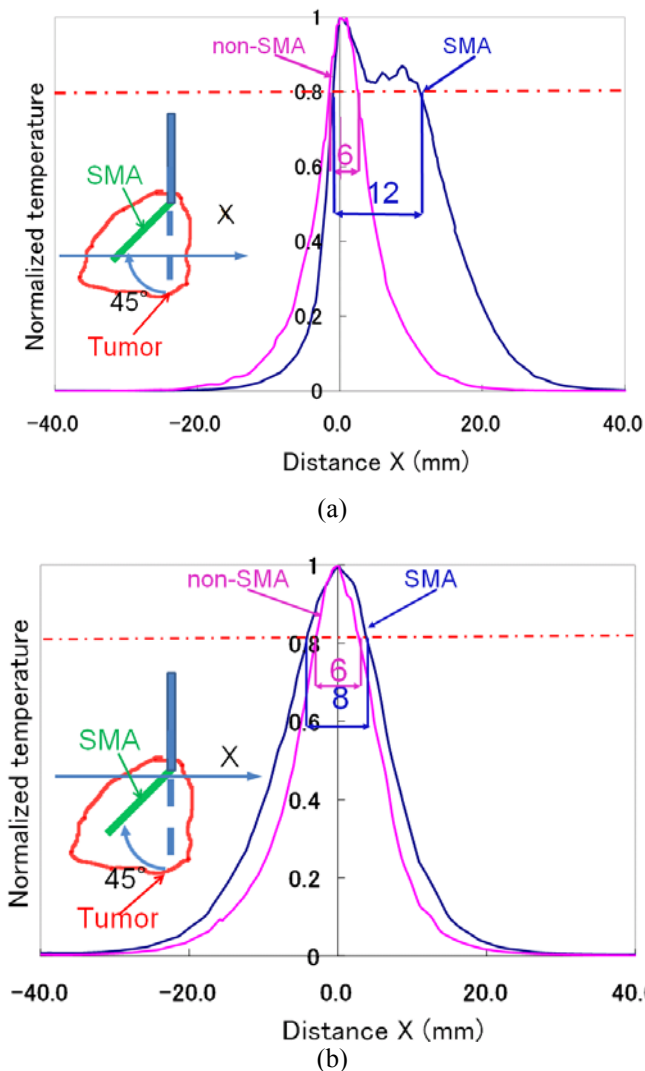


Fig. 9. Normalized temperature profiles on the x-axis:
 (a) on the top of needles,
 (b) on the bottom of needles.

shows the temperature distribution of the circumference of needles, bent to 0°, 22.5° and 45° angles under 30 seconds of heating respectively. Here, the normalized temperature T_N is given by the equation (7):

$$T_N = \frac{T - T_{\min}}{T_{\max} - T_{\min}} \quad (7)$$

Where T_{\min} is the minimum temperature on the x-axis, T_{\max} is the maximum temperature on the x-axis. Now, the minimum temperature is 37 °C and the maximum temperature is 43.5 °C. The temperature rise is 6.5 °C, then 42 °C is about 80% of the temperature rise. So, we discuss over the normalized temperature value of 0.8.

Fig. 9 shows the normalized temperature profiles along the x-axis. Fig. 9(a) shows the profiles on the top of the SMA

needle, and Fig. 9(b) shows the profiles on the bottom of the SMA needle. In Fig. 9(a), comparing non-shape memory function and shape memory function at the normalized temperature value of 0.8, the heated length is 6mm in the case of non-shape memory function. On the other hand, it is 12mm in the case of shape memory function. In Fig. 9(b), the heated length is 6mm in the case of non-shape memory function and is 8mm in the case of shape memory function.

In this paper, we presented a computer analysis of temperature distribution using the anatomical FEM model and the SMA needle type applicator.

From these results, it was confirmed that the proposed SMA needle type applicator could overcome the weak point and use on clinical heating.

V. CONCLUSION

We proposed a method of reconstructing the 3-D anatomical model from MRI and X-ray CT images. The results of computer simulations using the SMA needle type applicator for brain tumors were presented. According to our computer simulations, it was found that the proposed SMA needle type applicator could be used in clinical heating.

We are now constructing a method to practice an invasive hyperthermia treatment by Virtual Reality.

REFERENCES

- [1] K. Kato, J. Matuda, T. Yamashita, R. Tanaka, "Simultaneous estimation of blood flow rate and tissue temperature" *Frontiers of Med Biol Eng*, vol. 4, pp. 135-143, 1992
- [2] R.F Tumor "Regional hyperthermia with an annular phased array" *IEEE trans Biol Med Eng*, vol 31, no 1, pp. 106-114, 1984
- [3] T. Yabuhara, K. Kato, "Development of the re-entrant type resonant cavity applicator for brain tumor hyperthermia -Experimental heating results-", *Proc. of IEEE EMBS2006*
- [4] Ryo Miyata, Kazuo Kato, "Temperature Distributions of Developed Needle Type Applicator" , *Proc. of IEEE EMBS*, 6801, 2005.
- [5] Y. Kanazawa, K. Kato, T. Yabuhara, T. Uzuka, H. Takahashi and Y. Fujii "Improvement of Needle Type Applicator Made of Shape Memory Alloy", *Proc. of IEEE EMBS2008*
- [6] Ana O. Rodrigues, Juliano J. Viana, Luiz O.C. Rodrigues, Joao A. Vasconcelos, Jaime A. Ramirez Tim Green, Ernest M. Freeman, "3D Visualization of Temperature Distributions Induced by a Cellular Telephone in a Model of the Human Head", *Proc. of SBMO/IEEE MTT-S IMOC 2003*